



# Development of an electrochemical sensor for in-situ monitoring of reactive species produced by cold physical plasma

Zahra Nasri<sup>a,\*</sup>, Giuliana Bruno<sup>a</sup>, Sander Bekeschus<sup>a</sup>, Klaus-Dieter Weltmann<sup>b</sup>, Thomas von Woedtke<sup>b</sup>, Kristian Wende<sup>a,\*</sup>

<sup>a</sup> Center for Innovation Competence plasmatis, Leibniz Institute for Plasma Science and Technology, Greifswald, Germany

<sup>b</sup> Leibniz Institute for Plasma Science and Technology, Greifswald, Germany

## ARTICLE INFO

### Keywords:

Electrochemical sensors  
Reactive oxygen and nitrogen species  
Cold physical plasma  
Toluidine blue  
Hydrogen peroxide  
In-situ detection

## ABSTRACT

The extent of clinical applications of oxidative stress-based therapies such as photodynamic therapy (PDT) or respiratory chain disruptors are increasing rapidly, with cold physical plasma (CPP) emerging as a further option. According to the current knowledge, the biological effects of CPP base on reactive oxygen and nitrogen species (RONS) relevant in cell signaling. To monitor the safety and the biological impact of the CPP, determining the local generation of RONS in the same environment in which they are going to be applied is desirable. Here, for the first time, the development of an electrochemical sensor for the simple, quick, and parallel determination of plasma-generated reactive species is described. The proposed sensor consists of a toluidine blue redox system that is covalently attached to a gold electrode surface. By recording chronoamperometry at different potentials, it is possible to follow the in-situ production of the main long-lived reactive oxygen and nitrogen species like hydrogen peroxide, nitrite, hypochlorite, and chloramine with time. The applicability of this electrochemical sensor for the in-situ assessment of reactive species in redox-based therapies is demonstrated by the precise analysis of hydrogen peroxide dynamics in the presence of blood cancer cells.

## 1. Introduction

Several oxidative stress-based therapies, such as radiotherapy, chemotherapy, and photodynamic therapy, are specifically designed to increase reactive oxygen and nitrogen species (RONS) levels in cancer cells to induce their death through sudden and intense oxidative stress [1]. Cold physical plasma (CPP) produces similar levels of RONS with redox-based therapies. CPP is a near room temperature ionized gas, which is generated mostly by plasma jets or dielectric barrier discharges [2]. CPPs now pertain to a wide range of purposes in medicine, including cancer therapy [3–6], blood coagulation [7–9], chronic wound treatment and dermatology [10–12] and dental care [13–15]. It is assumed that long and short-lived RONS such as hydrogen peroxide (H<sub>2</sub>O<sub>2</sub>), ozone (O<sub>3</sub>), hydroxyl radical (•OH), superoxide (•O<sub>2</sub><sup>-</sup>), singlet oxygen (<sup>1</sup>O<sub>2</sub>), atomic oxygen (O), nitrogen dioxide radical (•NO<sub>2</sub>), peroxyxynitrite (ONOO<sup>-</sup>), and nitric oxide (•NO) generated by plasma are the critical elements in the above mentioned medical applications of CPPs [16–18]. The produced reactive species will deliver through the cutaneous and sub-cutaneous materials in contact with plasma jet into the specific cells

within the living tissues to interact with them and start a biochemical process [19]. Some of these processes can initiate or continue even after the CPP is switched off. These post-discharge reactions may contribute significantly to the biological effects induced by CPP [20].

Many parameters have an effect on the type and amount of produced reactive species by plasma, like physical specifications of the plasma source such as voltage and frequency, temperature, feed gas flow rate and composition, air humidity, and surrounding gas composition [21]. Using the argon-driven atmospheric-pressure plasma jet kINPen, a specific gas shielding device was designed to separate the plasma effluent from the atmospheric air and to modulate the surrounding gas by a specific gas curtain [22]. Lackmann et al. found that the usage of this curtain gas setup for the kINPen plasma jet and modulation of the feed gas conditions will increase the presence of nitrosative modifications on the thiol moiety of cysteine, which indicates more production of the reactive nitrogen species [23]. Also, the nature of the target in contact with the plasma has a significant effect on the plasma properties and, thus, on the production of reactive species. It is investigated that the permittivity and the conductivity of the target have a strong influence on

\* Corresponding authors.

E-mail addresses: [zahra.nasri@inp-greifswald.de](mailto:zahra.nasri@inp-greifswald.de) (Z. Nasri), [kristian.wende@inp-greifswald.de](mailto:kristian.wende@inp-greifswald.de) (K. Wende).

<https://doi.org/10.1016/j.snb.2020.129007>

Received 10 June 2020; Received in revised form 10 September 2020; Accepted 2 October 2020

Available online 7 October 2020

0925-4005/© 2020 The Authors.

Published by Elsevier B.V. This is an open access article under the CC BY-NC-ND license

(<http://creativecommons.org/licenses/by-nc-nd/4.0/>).

the plasma plume properties like the induced electric field, which leads to the intensive changes of the reactive species production compared to the freely expanding jet in the air [24–26]. Darny et al. reported that strong coupling between the characteristics of the plasma and target has a direct effect on the feed gas flow expansion over the target results in different mixing with ambient air, which is very important in reactive species production [27]. Also, the distance of the plasma source from the target and the target thickness can alter the chemical composition of the reactive species produced by jet [28]. Jablonowski et al. demonstrated that the density of the generated reactive oxygen species by the plasma is dependent on the distance of the target to the active plasma zone [29].

In plasma medicine, there are many targets with different physical and chemical properties, which affect the production of reactive species by plasma. It is appropriate to study plasma in the same environment in which it is going to be applied. It avoids the transposition of the results between the in-vitro and the in-vivo experiments that are carried out under diverse conditions. So a real-time in-situ control of plasma reactive species production is necessary. There are already many analytical methods for the detection of plasma produced liquid phase reactive species [30] like electron paramagnetic resonance spectroscopy for the detection of hydroxyl radicals [31], ozone and singlet delta oxygen [29] and nitric oxide [32], colorimetric or colorimetric/fluorometric assays for the detection of hydrogen peroxide [33,34] and peroxyxynitrite [35], spectroscopic detection of hydroxyl radicals, superoxide anion radicals [33,36] and hypochlorite [37], ion chromatography detection of nitrite and nitrate [23,38] and mass spectrometry analysis of hydroxyl radicals [39]. Although all of these methods can be applied for the measurement of reactive species with high sensitivity and low detection limits, it is not possible to employ them for in-situ measurements. For this propose, an electrochemical sensor is designed to follow the in-situ production of reactive species during plasma treatments. Electrochemical sensors are promising tools in the clinical analysis due to the fast analytical screening, possibility of in-situ detections, high selectivity, experimental simplicity, portability, and low cost [40,41]. Nowadays, there is a rapid expansion for electrochemical detection of redox species, especially hydrogen peroxide using advanced nanomaterials and conducting polymer composites [42–44]. However, due to the CPP features to produce a mixture of active agents including free charged particles, radicals, reactive species, UV radiation, and electromagnetic [16,18], the proposed electrochemical sensor is designed to have no cross-linking agent or complex matrices to avoid unwanted chemical reactions with plasma generated reactive entities. The proposed sensor is based on a toluidine blue (TB) modified electrode because of the well-known electrocatalytic behavior of toluidine blue [45–49]. Toluidine blue was immobilized on the surface of the gold screen-printed electrode directly by covalent bonds using diazonium chemistry to ensure the long-term stability compared to the poly(toluidine blue O) films [50]. The electrocatalytic behavior of the toluidine blue modified electrode for the redox reaction of long-lived reactive species produced by plasma in the liquid phase was studied. It was found that by recording chronoamperometry at different potentials, it is possible to follow the production of the main long-lived reactive species in a bulk liquid such as hydrogen peroxide, nitrite, hypochlorite, and chloramine [51] during plasma treatment. Finally, the cellular responses of blood cancer cell lines (Jurkat and THP-1 cells) exposed to CPP was investigated using the introduced sensor. The obtained results show that electrochemical sensors are appropriate devices that can be used in every medical plasma treatments to control the production and delivery of reactive species.

## 2. Experimental

### 2.1. Reagents

Toluidine blue (TB), hydrogen peroxide (30 % w/w), sodium nitrate, ammonia (anhydrous,  $\geq 99.9$  %) and 3,3',5,5'-tetramethylbenzidine ( $\geq 98.0$  %) were purchased from Sigma-Aldrich (Sigma-Aldrich Chemie

GmbH, Germany). Sodium hypochlorite (5% active chlorine) was from Acros organics (Fisher Scientific GmbH, Germany). Titanyl sulfate (5% Ti(IV) in sulfuric acid) was from Merck (Merck Chemicals GmbH, Germany). All other reagents were of analytical grade and used without further purification. All aqueous solutions were prepared with ultrapure water (Milli-Q® Merck KGaA, Germany). Argon gas (argon N50), nitrogen (nitrogen N50), and oxygen (oxygen N48) as feed gas of plasma jet were from Air Liquide (Air Liquide Deutschland GmbH, Germany).

### 2.2. Plasma source

The kINPen09 (neoplas tools GmbH, Germany) was used as a well characterized plasma source [52] running at 1.1 W and a frequency of 1 MHz. Argon was used as feed gas at a flux of 1.5 standard liters per minute (slm). In medical applications, the standard flow rate of the plasma feed gas is 3.0 slm. However, because of the high convection of the liquid in this flux, which can disturb in-situ electrochemical measurements, a lower feed gas flow rate was applied. Depending on the experiment, either pure argon (Ar), argon with an admixture of 1 % oxygen (Ar/O<sub>2</sub>), or 1 % nitrogen (Ar/N<sub>2</sub>) was used. All the experiments were carried out two times: under ambient air conditions or using a 2.5 slm N<sub>2</sub> as shielding gas for plasma effluent [22,53]. A volume of 750  $\mu\text{L}$  of phosphate-buffered saline (PBS) pH 7.4 were treated with the kINPEN at a distance of 9 mm between the jet nozzle and the sample surface.

### 2.3. Electrochemical measurements

Electrochemical measurements were carried out using a potentiostat AUTOLAB PGSTAT302 N (Deutsche METROHM GmbH & Co. KG, Germany) electrochemical system. Modified or unmodified gold screen-printed electrodes (SPEs) consisting of gold working and counter electrodes, and a silver reference electrode were used as standard three-electrode cell (refs. 220AT, DropSens, Spain). The chronoamperogram of the TB modified screen-printed electrode (TB/SPE) at different potentials were recorded during the treatment time.

### 2.4. Preparation of TB modified electrode

As TB is an aromatic amine, diazonium chemistry was used for the covalent attachment of TB molecules to the electrode surface. For the in-situ generation of TB diazonium salt, an ice-cold sodium nitrite aqueous solution was added drop by drop to a solution of TB in 0.5 M HCl. Final concentrations of TB and sodium nitrite were 1 mM and 2 mM, respectively [54]. Then 200  $\mu\text{L}$  of this solution was added to the electrochemical cell consisting of gold SPE and was derivatized by cyclic voltammetry scanning from 0 to  $-0.35$  V at  $100$   $\text{mV s}^{-1}$  scan rate for five scans. Finally, the modified electrode was rinsed with water several times to remove the loosely adsorbed TB molecules.

### 2.5. Cell culture

Cell related experiments were performed with Jurkat T cells, an immortalized line of human CD4 + T lymphocyte cells (DSMZ, Germany), and THP-1 cells, a human monocytic cell line derived from an acute monocytic leukemia patient (CLS, Germany), as previously described [55]. Briefly, cells were cultivated in Roswell Park Memorial Institute (RPMI) 1640 medium supplemented with either 8% (Jurkat) or 10 % (THP-1) fetal bovine serum, 2 mM L-glutamine, 0.1  $\text{mg L}^{-1}$  streptomycin, and 100  $\text{U mL}^{-1}$  penicillin (Sigma-Aldrich Chemie GmbH, Germany) at 37 °C in 95 % relative humidity and 5% CO<sub>2</sub> (Binder, Germany).

### 2.6. Raman studies

Raman spectroscopy studies were done using a Raman spectrometer capable of Raman microscopy in combination with an inverted

microscope (inVia with Leica DMI 3000 M, Renishaw, Germany). Detailed parameters were argon laser with 532 nm laser excitation and 0.5 % laser power, exposition time of 10 s, grating with 2400 grooves  $\text{cm}^{-1}$  scanning in the region of 0 to 3500  $\text{cm}^{-1}$ .

## 2.7. Colorimetric assays

To compare the results obtained from TB modified gold SPE with other standard methods, hydrogen peroxide and hypochlorite concentrations were determined via colorimetric assay. The amount of produced hypochlorite is of great importance, while it is related to the level of atomic oxygen induction in PBS. Atomic oxygen is delivered to the solution by plasma and can oxidize  $\text{Cl}^-$  to  $\text{ClO}^-$  [56].

For hydrogen peroxide measurements, a volume of 100  $\mu\text{L}$  of the sample was incubated with 200  $\mu\text{L}$  of reagent, consisting of a solution of titanil sulfate ( $\text{TiOSO}_4$ , 5% Ti(IV) in sulfuric acid) in a 96 well-plate for 15 min. Indeed, in aqueous acidic solutions, Ti(IV) and hydrogen peroxide react to form pertitanic acid ( $\text{H}_2\text{TiO}_4$ ), which can be quantified at 407 nm through a spectrophotometer (Infinite M200 Pro plate reader, Tecan Group Ltd., Switzerland) after the analysis of a calibration curve. For each sample (triplicates), two technical replicates were performed (duplicates), for a total of 6 measurements per sample [57].

Hypochlorite concentrations were measured using TMB (3,3',5,5'-tetramethylbenzidine) assay. A volume of 80  $\mu\text{L}$  of 200 mM sodium acetate buffer solution (pH 4.0) was added to 120  $\mu\text{L}$  of 5 mM TMB in  $\text{H}_2\text{O}$ : ethanol (1:1) in a 96 well-plate. At last, 100  $\mu\text{L}$  of samples were incubated with the reaction solutions up to 15 min. The absorbance was read at 655 nm at 5 and 15 min, and the values for 5 min was used to exclude time-related specific reactions and disruption of the dye. A calibration curve was build using 10 points starting from 700  $\mu\text{M}$  of hypochlorite [58].

## 2.8. Ion chromatography

The concentration of nitrite in samples were determined by ion chromatography (ICS-5000, Dionex Corp., USA). Before injection (10  $\mu\text{L}$ ), all the samples were diluted three fold by adding ultrapure water. An IonPac® AS23 pre-column (2  $\times$  50 mm, Thermo Fisher Scientific Inc., USA) coupled to an IonPac® AS23 anion exchange column (2  $\times$  250 mm, Thermo Fisher Scientific Inc., USA) was used for separation in an isocratic mobile phase (4.5 mM  $\text{Na}_2\text{CO}_3$ /0.8 mM  $\text{NaHCO}_3$ ) regime and 250  $\mu\text{L min}^{-1}$  flow rate. The analyte was detected by conductivity and UV detection (210 nm).

## 3. Results and discussion

### 3.1. Sensor preparation and characterization

Scheme 1 represents the strategy used for the synthesis and electrografting of TB diazonium salt onto the gold electrode. The bonding of TB molecules onto the electrode surface was carried out by the



Scheme 1. Synthesis and electrografting of TB diazonium salt onto the gold SPE.

electrochemical reduction of the in-situ generated diazonium salt. Recording repetitive cyclic voltammograms (CVs) under in-situ conditions led to the attachment of TB molecules to the gold surface. As is shown in Fig. 1A, the first CV has a broad irreversible peak at  $E_p = -0.2$  V, which is related to the irreversible reaction of losing dinitrogen and the formation of radicals on the electrode surface. In the following scans, the peak disappears completely due to the covalent attachment of highly reactive radicals to the gold electrode, which blocks further reduction of diazonium salt [59,60]. Fig. 1B shows the CV of the TB modified electrode in PBS solution pH 7.4, after washing the electrode with water for several times. The resulting CV presents a well-defined reversible peak attributed to the redox reaction of bonded TB molecules.

To prove the existence of TB molecules on the surface of the modified electrode, Raman spectra of gold electrodes were recorded before and after modification with TB (Fig. 2). Several strong Raman bands, observed mainly within the frequency region of 1000–1700  $\text{cm}^{-1}$ , indicate that TB is successfully attached to the surface of the electrode. The high frequency spectral region ranging from 1650 to 1300  $\text{cm}^{-1}$  presents mainly skeletal ring stretching vibrations. From these, the band at 1502  $\text{cm}^{-1}$  could be ascribed to the aromatic ring C–C stretching mode [61]. The intense peak near 1625  $\text{cm}^{-1}$  belongs to the aromatic ring stretching vibration of short C=C bonds coupled with stretching vibration of C–N [62]. Mid-intense in-plane C–H bending vibrations coupled with C–S–C stretching motion is attributed to the observed peak at 1151  $\text{cm}^{-1}$  [61].

### 3.2. Quantification of simultaneously present long-lived RONS by TB/SPE

In clinical plasma applications, various short and long-lived RONS will be created across the plasma-liquid interface within or surrounding the target, which will then propagate towards and diffuse through it [63]. Besides, most of the short-lived reactive species will end up in the form of long-lived chemical products [20,64]. So, the measurement of the long-lived reactive species is of considerable interest. In the following, the application of the TB/SPE toward the measurement of long-lived plasma generated RONS ( $\text{H}_2\text{O}_2$ ,  $\text{O}_3$ ,  $\text{O}_2^-$ ,  $\text{NO}_2^-$ ,  $\text{NO}_3^-$ ,  $\text{ClO}^-$ , and  $\text{NH}_2\text{Cl}$ ) was studied to identify which one is detectable by the proposed sensor.

#### 3.2.1. Oxidation of nitrite on TB/SPE

The electrocatalytic behavior of TB modified gold SPE toward oxidation of nitrite was investigated by cyclic voltammetry. Fig. 3A shows the CVs of unmodified and TB modified gold SPEs in PBS pH 7.4 in the absence and presence of different concentrations of  $\text{NaNO}_2$  recorded at 10  $\text{mV s}^{-1}$ . As is shown in Fig. 3A, by increasing the concentration of  $\text{NaNO}_2$ , the oxidation peak significantly starts to grow at ca. 0.60 V to reach a maximum at 0.70 V. By comparison to the unmodified SPE, the signal is slightly shifted toward lower overpotentials, suggesting a favorable electrocatalytic effect due to the presence of TB molecules

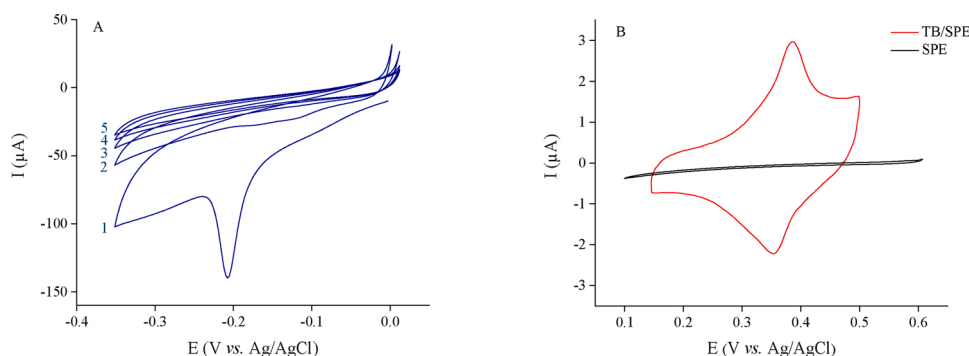


**Fig. 1.** Repetitive cyclic voltammograms of the electrochemical reduction of in-situ generated TB diazonium salt on gold SPE using scan rate of  $100 \text{ mV s}^{-1}$  (A). Cyclic voltammograms of unmodified and TB modified SPEs in PBS solution (pH 7.4) at scan rate of  $100 \text{ mV s}^{-1}$  (B).

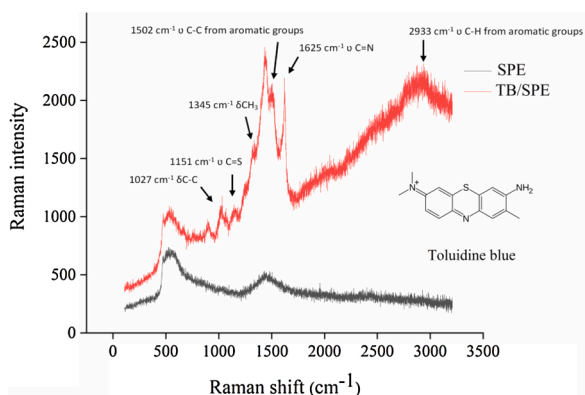


**Fig. 2.** Raman spectra of unmodified and TB modified gold SPEs.  $\delta$  denotes a bending vibration and  $\nu$  denotes a stretching vibration.

onto the electrode surface [48]. So the TB modified electrode has excellent electrocatalytic properties and facilitates the lower potential amperometric measurement of  $\text{NaNO}_2$ . The chronoamperogram of TB modified electrode in PBS pH 7.4, at  $E = 0.70 \text{ V}$  vs. Ag/AgCl was recorded, and based on that, the calibration curve was plotted (Fig. 3B). The calibration plot is linear over the concentration range of 0.01–4.0 mM of  $\text{NaNO}_2$ .

### 3.2.2. Oxidation of hydrogen peroxide on TB/SPE

The recorded CVs of unmodified and TB modified SPEs in PBS pH 7.4 in the absence and presence of 1 mM of  $\text{H}_2\text{O}_2$  (Fig. 4A) suggest a typical electrocatalytic oxidation process (EC'), which confirm that TB molecules can catalyze the oxidation reaction of  $\text{H}_2\text{O}_2$ . For this, hydrogen peroxide will be oxidized by reducing the oxidized TB molecules on the

surface of the electrode. The calibration curves for measurement of  $\text{H}_2\text{O}_2$  at  $E = 0.50 \text{ V}$  with a linear range of 0.02–2.0 mM and at  $E = 0.70 \text{ V}$  with a linear range of 0.01–2.0 mM were plotted using chronoamperometry technique (Fig. 4B).

### 3.2.3. Reduction of hypochlorite on TB/SPE

The TB modified gold SPE also shows electrocatalytic behavior toward the reduction of NaClO. Hypochlorite will be reduced to chloride by oxidizing the reduced form of TB. The recorded CVs of the unmodified and TB modified SPEs in the absence and presence of different concentrations of NaClO (Fig. 5A) support that it is possible to follow the production of hypochlorite by this modified electrode. The calibration curves at  $E = 0.30 \text{ V}$  with linear range of 0.02–3.0 mM and at  $E = 0.05 \text{ V}$  with linear range of 0.01–3.0 mM (Fig. 5B) were plotted. This is the first report in which toluidine blue serves as an electrochemical mediator for the measurement of hypochlorite. The obtained results indicate the capability of this sensor for the sensitive detection of hypochlorite in a wide concentration range.

### 3.2.4. Reduction of chloramine on TB/SPE

Chloramine was synthesized in-situ from the reaction of  $\text{NH}_3$  and NaClO in PBS pH 8.0, based on the following reaction (reaction 1).



By taking advantage of the low reactivity of  $\text{NH}_2\text{Cl}$  in alkaline solution,  $\text{NH}_2\text{Cl}$  formation has a preference to free  $\text{NH}_3$ , so 1 mol of  $\text{NH}_2\text{Cl}$  will be produced from 1 mol of  $\text{ClO}^-$  [65].  $\text{NH}_2\text{Cl}$  production was investigated via following the changes in the concentration of 1 mM NaClO by adding 1 mM  $\text{NH}_3$  and plotting chronoamperogram at  $E = 0.30 \text{ V}$ . As is shown in the inset of Fig. 6A, adding NaClO to the electrochemical cell results in a current related to the electrocatalytic reduction of  $\text{ClO}^-$  at TB modified electrode. This current was

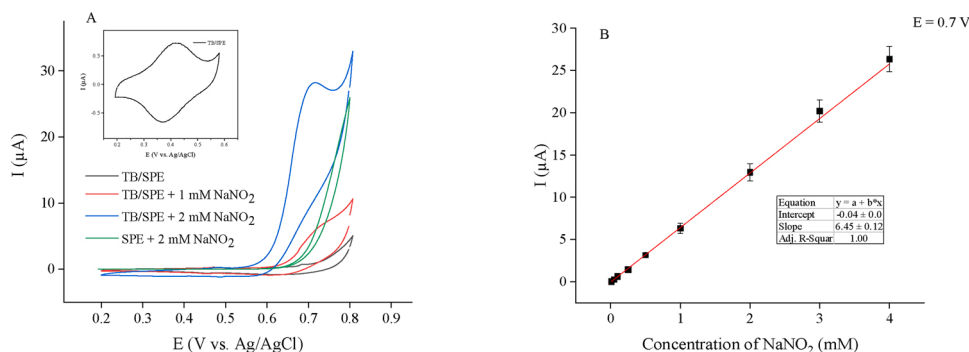


**Fig. 3.** Cyclic voltammograms of unmodified and TB modified SPEs in PBS pH 7.4, in the absence and presence of different concentrations of  $\text{NaNO}_2$  recorded at  $10 \text{ mV s}^{-1}$ , inset: cyclic voltammogram of TB modified SPE recorded at  $10 \text{ mV s}^{-1}$  (A). Calibration curve plotted based on current-time response of TB modified SPE in PBS (pH 7.4) at 0.70 V vs. Ag/AgCl for successive addition of  $\text{NaNO}_2$  (B). Triplicates ( $n = 3$ ) with standard deviation are shown.

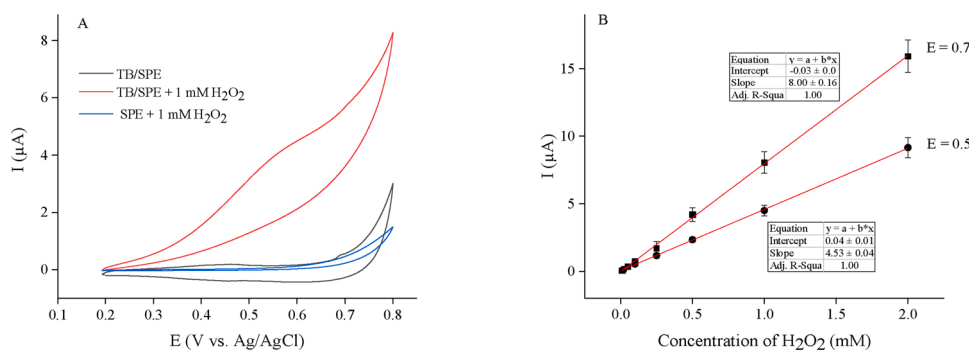


**Fig. 4.** Cyclic voltammograms of unmodified and TB modified SPEs in PBS pH 7.4, in the absence and presence of 1 mM of H<sub>2</sub>O<sub>2</sub> recorded at 10 mV s<sup>-1</sup> (A). Calibration curve plotted based on current-time response of TB modified SPE in PBS (pH 7.4) at 0.50 V and 0.70 V vs. Ag/AgCl for successive addition of H<sub>2</sub>O<sub>2</sub> (B). Triplicates (n = 3) with standard deviation are shown.

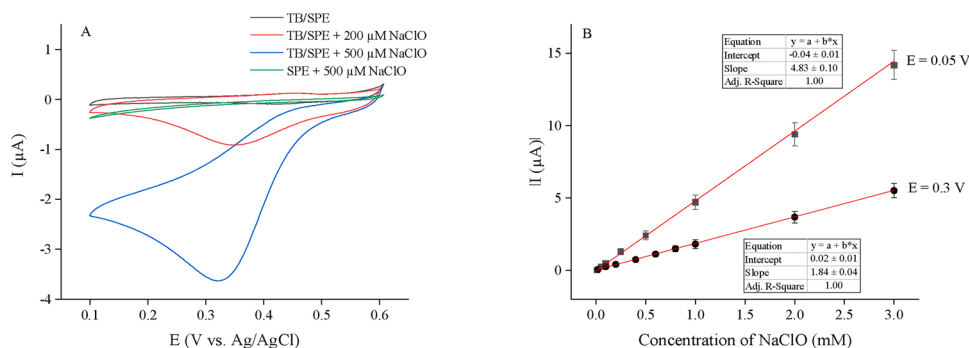


**Fig. 5.** Cyclic voltammograms of unmodified and TB modified SPEs in PBS pH 7.4, in the absence and presence of different concentrations of NaClO recorded at 10 mV s<sup>-1</sup> (A). Calibration curve plotted based on current-time response of TB modified SPE in PBS (pH 7.4) at 0.30 V and 0.05 V vs. Ag/AgCl for successive addition of NaClO (B). Triplicates (n = 3) with standard deviation are shown.

disappeared nearly completely by the addition of NH<sub>3</sub>, which is related to the consumption of ClO<sup>-</sup> and formation of NH<sub>2</sub>Cl inside the electrochemical cell. NH<sub>2</sub>Cl is not electroactive at E = 0.30 V, but it is possible to follow its production at E = 0.05 V (Fig. 6A). The electrocatalytic behavior of TB molecules for the reduction of NH<sub>2</sub>Cl was investigated by recording CVs of unmodified and TB modified SPEs in PBS pH 8.0 in the absence and presence of different concentrations of NH<sub>2</sub>Cl (Fig. 6A). By plotting chronoamperometry at E = 0.05 V, the calibration curve for the reduction of NH<sub>2</sub>Cl to ammonium was plotted (Fig. 6B) with a linear range of 0.01–3.0 mM.

Fast and sensitive measurement of chloramine is critical, as it is going to be the final disinfectant instead of chlorine disinfection in drinking water systems [66]. Here, for the first time, an electrochemical sensor is introduced for the detection of chloramine. The proposed sensor would also facilitate chloramine measurements in water supply networks.

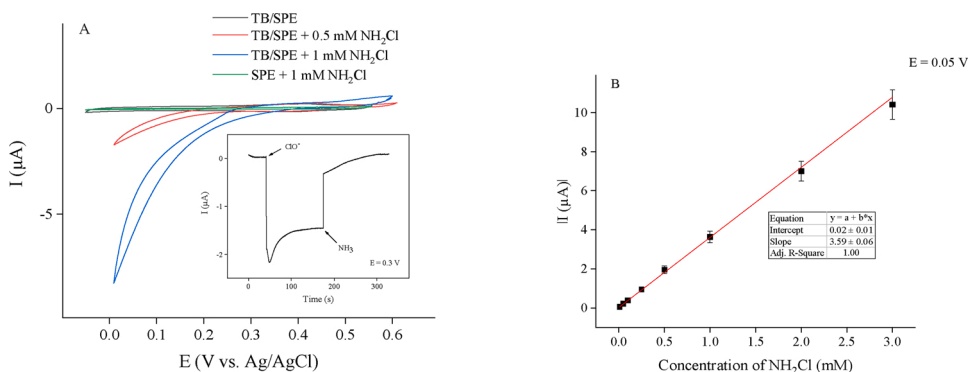


**Fig. 6.** Cyclic voltammograms of unmodified and TB modified SPEs in PBS pH 8.0, in the absence and presence of different concentrations of NH<sub>2</sub>Cl recorded at 10 mV s<sup>-1</sup>, inset: following the production of NH<sub>2</sub>Cl by recording current-time response of 1 mM NaClO after adding 1 mM NH<sub>3</sub> in PBS (pH 8.0) at 0.30 V vs. Ag/AgCl using TB modified SPE (A). Calibration curve plotted based on current-time response of TB modified SPE in PBS (pH 8.0) at 0.05 V vs. Ag/AgCl for different concentration of NH<sub>2</sub>Cl (B). Triplicates (n = 3) with standard deviation are shown.

All parameters corresponding to the amperometric detection of NO<sub>2</sub><sup>-</sup>, H<sub>2</sub>O<sub>2</sub>, ClO<sup>-</sup> and NH<sub>2</sub>Cl by TB modified SPE are summarized in Table 1.

### 3.2.5. Oxidation of superoxide, nitrate, and ozone on TB/SPE

The determination of superoxide in the presence of hydrogen

**Table 1**

Analytical parameters corresponding to the amperometric detection of NaNO<sub>2</sub>, H<sub>2</sub>O<sub>2</sub>, NaClO and NH<sub>2</sub>Cl by TB/SPE.

Analyte	Potential V	Sensitivity μA/mM	Detection limit μM	Linear range mM
NaNO <sub>2</sub>	0.70	6.45	4.0	0.01 – 4.0
H <sub>2</sub> O <sub>2</sub>	0.50	4.53	10.0	0.02 – 2.0
NaClO	0.30	1.84	10.0	0.02 – 3.0
NH <sub>2</sub> Cl	0.05	3.59	5.0	0.01 – 3.0

peroxide is not possible due to the hydrolysis and disproportionation of superoxide to hydrogen peroxide in water. Different concentrations of nitrate and ozone produced by laboratory Ozonizer 301.7 (Erwin Sander Elektroapparatebau GmbH, Germany) inside the solution were tested. The absence of the related signal indicates that TB modified SPE cannot catalyze the redox reaction of nitrate and ozone. So it is not possible to follow their production using the proposed sensor.

### 3.3. In-situ following of reactive species produced by CPP

Selective determination of the amount of produced  $\text{NO}_2^-$ ,  $\text{H}_2\text{O}_2$ ,  $\text{ClO}^-$  and  $\text{NH}_2\text{Cl}$  during plasma treatment is possible by recording chronoamperograms at potentials of 0.70 V, 0.50 V, 0.30 V and 0.05 V vs. Ag/AgCl respectively, based on the following equations:

$$\text{H}_2\text{O}_2: C_{\text{H}_2\text{O}_2} = (I_{E=0.5\text{V}} - 0.04) / 4.53 \quad (1)$$

$$\text{NO}_2^-: C_{\text{NO}_2^-} = (I_{E=0.7\text{V}} - (8.00 C_{\text{H}_2\text{O}_2} - 0.03)) + 0.04 / 6.45 \quad (2)$$

$$\text{ClO}^-: C_{\text{ClO}^-} = (I_{E=0.3\text{V}} - 0.020) / 1.84 \quad (3)$$

$$\text{NH}_2\text{Cl}: C_{\text{NH}_2\text{Cl}} = (I_{E=0.05\text{V}} - (4.83 C_{\text{ClO}^-} - 0.04)) - 0.02 / 3.59 \quad (4)$$

At the potential of 0.50 V, the only species which has an electrochemical reaction is hydrogen peroxide. By recording chronoamperometry at 0.50 V and using the  $\text{H}_2\text{O}_2$  calibration curve at this potential, the concentration of the produced hydrogen peroxide was determined (eq. 1). To follow changes in nitrite concentration, chronoamperometry at 0.70 V was recorded. But at this potential,  $\text{H}_2\text{O}_2$  also will be oxidized. The amount of the produced  $\text{H}_2\text{O}_2$  during plasma treatment is known from eq. 1. Using the calibration curve of  $\text{H}_2\text{O}_2$  at  $E = 0.70\text{V}$ , the generated current by hydrogen peroxide at this potential was calculated. By subtracting the part of the hydrogen peroxide from the produced current of chronoamperometry at 0.70 V, the concentration of nitrite was measured (eq. 2). The same is for the reduction of hypochlorite and chloramine. The amounts of generated hypochlorite during plasma treatment was calculated using chronoamperometry at 0.30 V and based on its calibration curve at this potential (eq. 3). Chloramine production was followed at 0.05 V, but the recorded current at this potential belongs to the reduction of both hypochlorite and chloramine. The part of the hypochlorite in the produced current at 0.05 V was determined from its concentration (eq. 3) and calibration curve at 0.05 V, which must be subtracted from the generated current at 0.05 V to calculate the concentration of chloramine (eq. 4). The selectivity of the TB modified electrode for the determination of  $\text{NaNO}_2$ ,  $\text{H}_2\text{O}_2$ ,  $\text{NaClO}$ , and  $\text{NH}_2\text{Cl}$  in two synthetic mixtures with 100  $\mu\text{M}$  and 200  $\mu\text{M}$  concentration of each species were studied. The obtained recovery values for each analyte indicate the proposed sensor's capability for the selective determination of each species at the related potential (Table 2).

For in-situ following of reactive species produced by CPP, the production of  $\text{NO}_2^-$ ,  $\text{H}_2\text{O}_2$ ,  $\text{ClO}^-$  and  $\text{NH}_2\text{Cl}$  during treatment of 750  $\mu\text{L}$  of PBS pH 7.4 with Ar jet, in the absence (Fig. 7A) and presence (Fig. 7B) of shielding gas, was investigated. As is shown, without using shielding gas, a high concentration of  $\text{H}_2\text{O}_2$  was produced during treatment,

**Table 2**

Determination of  $\text{NaNO}_2$ ,  $\text{H}_2\text{O}_2$ ,  $\text{NaClO}$ , and  $\text{NH}_2\text{Cl}$  in synthetic mixtures by TB/SPE.

Analyte	Added ( $\mu\text{M}$ )	Found ( $\mu\text{M}$ )	Recovery (%)
$\text{NaNO}_2$	100	104.2 ( $\pm 3.7$ ) <sup>a</sup>	104.2
	200	207.4 ( $\pm 6.1$ )	103.7
$\text{H}_2\text{O}_2$	100	97.6 ( $\pm 2.8$ )	97.6
	200	204.9 ( $\pm 5.5$ )	102.5
$\text{NaClO}$	100	98.1 ( $\pm 3.2$ )	98.1
	200	195.5 ( $\pm 6.5$ )	97.8
$\text{NH}_2\text{Cl}$	100	103.8 ( $\pm 4.5$ )	103.8
	200	208.7 ( $\pm 6.9$ )	104.4

<sup>a</sup> The figures in parenthesis are standard deviation for three measurements.

which was decreased when the effluent was covered with  $\text{N}_2$  gas. When the plasma jet is utilized without shielding gas, ambient air species, as well as humidity particles diffuse into the active effluent of the plasma jet to produce higher concentrations of reactive species [67]. Also, the feed gas humidity is a vital parameter that has an effect on the amount of produced reactive species, especially OH radicals and  $\text{H}_2\text{O}_2$  [34]. The shielding gas curtain forms a cover to protect the effluent from ambient species diffusion. So, it is possible to control the surrounding atmosphere around the active effluent region to produce less reactive species during plasma treatment [22,53]. The air penetration inside the plasma effluent profoundly affects the plasma chemistry, which has great importance for biomedical applications.

By adding 1%  $\text{O}_2$  to the Ar feed gas, the type and amount of produced reactive species were altered. The production of  $\text{NO}_2^-$ ,  $\text{H}_2\text{O}_2$ ,  $\text{ClO}^-$  and  $\text{NH}_2\text{Cl}$  during treatment with Ar + 1%  $\text{O}_2$  plasma jet were followed without (Fig. 8A) and with (Fig. 8B)  $\text{N}_2$  shielding gas. The obtained results prove that, when the effluent of plasma was covered with  $\text{N}_2$  gas, a higher concentration of  $\text{ClO}^-$  and lower amounts of  $\text{H}_2\text{O}_2$  and  $\text{NO}_2^-$  were produced. This indicates when applying shielding gas, atomic oxygen from plasma effluent transfer directly to the sample and chloride ions in chloride-rich solutions such as PBS behave as a scavenger for atomic oxygen to form  $\text{ClO}^-$  [29,68]. Reaction 2 shows the main pathway leading to  $\text{ClO}^-$  formation in oxygen-containing plasmas [56]:



It is reported that dry oxygen-rich plasma is the only jet, which induces apoptosis in THP-1 leukaemia cells suggesting hypochlorous acid responsible for the observed effect [69]. So the working conditions have a significant impact on the type and amount of generated RONS.

By replacing the admixture gas with  $\text{N}_2$  (Fig. 9A and B), the generated RONS were changed. The results show that when the jet was working without shielding gas, a high concentration of  $\text{H}_2\text{O}_2$  was produced during treatment, but there is no sign of production of  $\text{NH}_2\text{Cl}$ . On the other hand, when the effluent was covered with  $\text{N}_2$  shielding gas, the produced reactive species replaced mostly with  $\text{NH}_2\text{Cl}$ . There is only one report on the production of  $\text{NH}_2\text{Cl}$  during plasma treatment [70], Maheux et al. observed a fast and efficient inactivation of *E. coli* suspensions which was achieved only with  $\text{He}/\text{N}_2$  cold physical plasma under  $\text{N}_2$  controlled atmosphere, whereas He and  $\text{He}/\text{O}_2$  treatments only led to limited and time-delayed inactivation. They connected the inactivation efficiency of  $\text{He}/\text{N}_2$  plasma to the preferential formation of  $\text{NH}_2\text{Cl}$  from the reaction of  $\text{NH}_4^+/\text{NH}_3$  with hypochlorite species. Production of ammonium in plasma treated solutions is via a two-step mechanism: dissociation of excited water molecules to hydrogen gas, and then the reaction of hydrogen with nitrogen present in the plasma phase and acid-base reaction in the liquid (reactions 3–6) [70]. Another mechanism for the formation of  $\text{NH}_2\text{Cl}$  is the reaction of produced  $\text{NH}_3$  with  $\text{Cl}_2$  (reactions 7 and 8). It is clear that by changing the conditions of Ar/ $\text{N}_2$  plasma treatment, one can replace the production of  $\text{H}_2\text{O}_2$  with  $\text{NH}_2\text{Cl}$ .



To compare the obtained results of TB modified gold SPE with standard methods, 750  $\mu\text{L}$  of PBS was treated for 3 min in the same conditions. The calculated concentrations of hydrogen peroxide and hypochlorite from colorimetric assay and nitrite from ion chromatography are shown in Fig. 10, which are in good agreement with the results

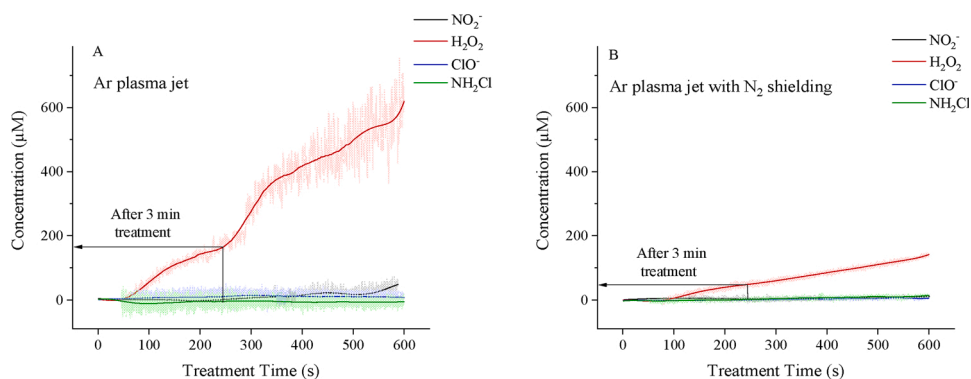


**Fig. 7.** In-situ measurement of the concentration of produced  $\text{NO}_2^-$ ,  $\text{H}_2\text{O}_2$ ,  $\text{ClO}^-$  and  $\text{NH}_2\text{Cl}$  during plasma treatment with 1.5 slm Ar jet under ambient air conditions without shielding gas (A) and with  $\text{N}_2$  shielding gas (B).

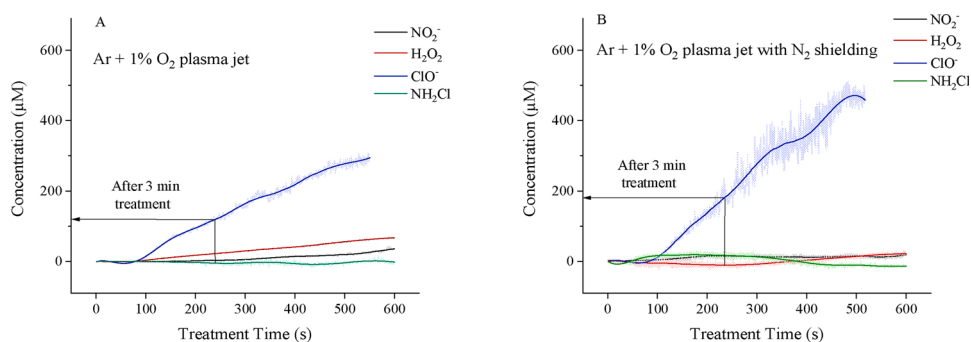


**Fig. 8.** In-situ measurement of the concentration of produced  $\text{NO}_2^-$ ,  $\text{H}_2\text{O}_2$ ,  $\text{ClO}^-$  and  $\text{NH}_2\text{Cl}$  during plasma treatment with 1.5 slm Ar + 1%  $\text{O}_2$  jet without shielding gas (A) and with  $\text{N}_2$  shielding gas (B).

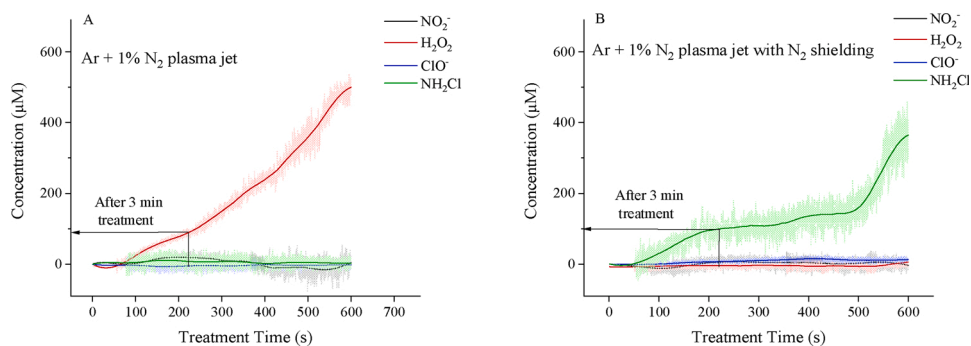


**Fig. 9.** In-situ measurement of the concentration of produced  $\text{NO}_2^-$ ,  $\text{H}_2\text{O}_2$ ,  $\text{ClO}^-$  and  $\text{NH}_2\text{Cl}$  during plasma treatment with 1.5 slm Ar + 1%  $\text{N}_2$  jet without shielding gas (A) and with  $\text{N}_2$  shielding gas (B).

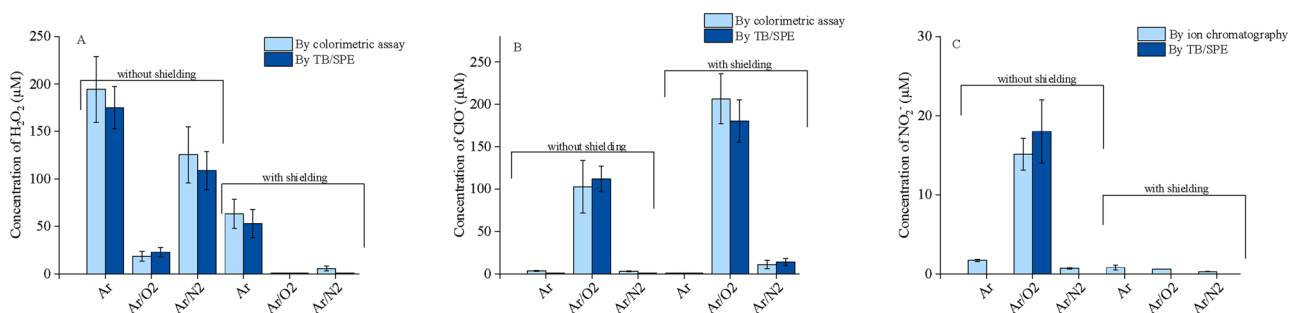


**Fig. 10.** Concentration of  $\text{H}_2\text{O}_2$  (A) and  $\text{ClO}^-$  (B) measured by colorimetric assay and  $\text{NO}_2^-$  (C) measured by ion chromatography in comparison with the concentrations obtained by TB/SPE after 3 min plasma treatment of 750  $\mu\text{L}$  PBS with a flow rate of 1.5 slm. Triplicates ( $n = 3$ ) with standard deviation are shown.

recorded by the proposed sensor.

### 3.4. Reactive species dynamics in the presence of blood cancer cells

The performance of the introduced sensor for practical applications was investigated in the presence of two leukemia cell lines of Jurkat and THP-1 cells. As hydrogen peroxide is an essential signaling molecule in cancer cells, the concentration of produced hydrogen peroxide during and after plasma treatment of two types of blood cancer cells was monitored by recording chronoamperometry at  $E = 0.50$  V in a PBS solution containing cancer cells. For plasma treatment,  $1.5 \times 10^5$  cells in 750  $\mu$ L PBS were treated with Ar feed gas 1.5 slm. The production of hydrogen peroxide during 3 min exposure to plasma and the changes in its concentration for 30 min after the plasma treatment was recorded using TB modified electrode (Fig. 11). The obtained results show that the effect of plasma treatment is entirely different for these two cell lines. The concentration of produced hydrogen peroxide in PBS containing THP-1 cells decreases after CPP treatment, which indicates these cells are consuming parts of the produced hydrogen peroxide. Unlike the THP-1 cells, the Jurkat cells produce even more hydrogen peroxide after the treatment.

The selective anti-tumor mechanism of CPP involves the inactivation of the protective membrane-associated catalase molecules of cancer cells trigger by singlet oxygen. After this initial step, cell-generated reactive species have a significant role in inactivating protective catalase, depleting glutathione, and initiating apoptosis-inducing RONS signaling [71]. Schmidt et al. reported that Jurkat cells have a very higher sensitivity to Ar plasma compared to THP-1 cells, as the number of transcripts tightly linked to molecules of the antioxidant defense system such as catalase (+5.38-fold) and glutathione peroxidases (+5.01-fold) is significantly elevated in THP-1 cells [72]. Based on that, THP-1 cells can protect themselves from endogenous oxidants and complete inactivation of the related protective catalase molecules. So, the decomposition of the generated hydrogen peroxide by catalase molecules of THP-1 cells is associated with the observed decay in Fig. 11. In case of Jurkat cells, optimal inactivation of catalase molecules happen. It is reported that short-lived RONS from CPP may activate cells to produce  $H_2O_2$ , which may trigger immune attack on tumorous tissues via the  $H_2O_2$ -mediated lymphocyte activation [73]. The generation of  $H_2O_2$  by Jurkat cells after plasma treatment increases the concentration of measured hydrogen peroxide. Cytotoxicity of the TB modified screen-printed electrode to the cancer cells was found to be negligible. Jurkat cells were challenged for 72 h with extracts of the gold SPE with or without toluidine blue modification. No significant differences to medium control were observed for either static extracts obtained in the electrochemical cell nor for shaking the complete sensor chip overnight (two-sided ANOVA/Tukey's test,  $p$ -value  $\geq 0.1$  for all conditions) (Fig. 12).

## 4. Conclusion

A simple, stable, and portable electrochemical sensor is described here based on the direct covalent attachment of TB molecules onto the electrode surface. This sensor has the ability to follow the real-time, in-situ production of long-lived reactive species output of plasma. The generated concentrations of nitrite, hydrogen peroxide, hypochlorite, and chloramine could be measured during plasma treatment by recording chronoamperograms at potentials of 0.70 V, 0.50 V, 0.30 V, and 0.05 V respectively. The introduced sensor also can monitor the post-discharge reactions, which may contribute significantly to the biological effects induced by cold physical plasma. Also, based on the knowledge on which species are essential for the desired plasma application, we can promote the formation of these species in the sample by changing plasma source design and get closer to achieve selectivity in plasma applications.

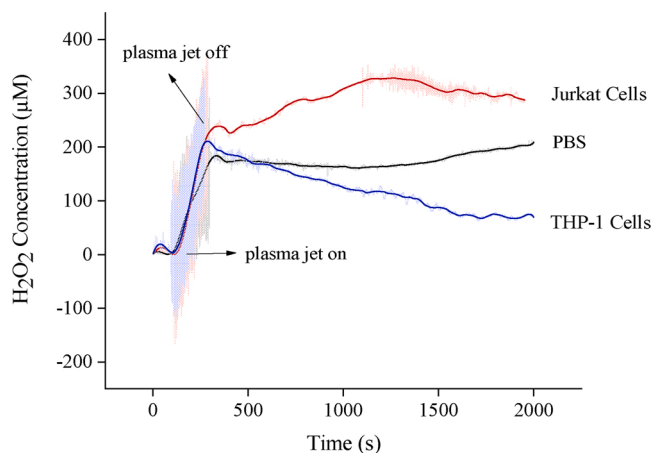


Fig. 11. In-situ measurement of the concentration of hydrogen peroxide during 3 min exposure to Ar plasma jet 1.5 slm, and for 30 min after the treatment in Jurkat and THP-1 cell lines and in PBS (pH 7.4).

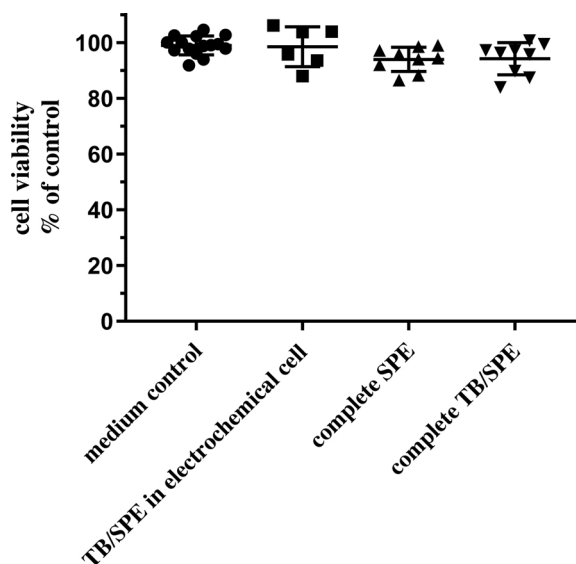


Fig. 12. Cytotoxicity test of the TB modified gold screen-printed electrode to the cancer cells. Jurkat cells were challenged for 72 h with extracts of the SPE with or without toluidine blue modification for static extracts obtained in the electrochemical cell or for shaking the complete sensor chip overnight (two-sided ANOVA/Tukey's test,  $p$ -value  $\geq 0.1$  for all conditions).

## Author contributions statement

Z.N., T. von W., and K.W. conceived and designed the experiments. Z.N. performed all electrochemical experiments. G.B. designed and performed ion chromatography and wet chemistry assays. S.B. designed the cell related experiments. All authors discussed the results. Z.N. and K.W. conceived and wrote the main manuscript and prepared all figures. All authors reviewed the manuscript.

## Declaration of Competing Interest

The authors report no declarations of interest.

## Acknowledgements

The authors are grateful to Felix Nießner for preparing cancer cell lines. We also thank Manuela Wende for testing the biocompatibility of the sensor chips. This work is funded by the German Federal Ministry of

Education and Research (BMBF) (grant numbers 03Z22DN12 and 03Z22DN11).

## Appendix A. Supplementary data

Supplementary material related to this article can be found, in the online version, at doi:<https://doi.org/10.1016/j.snb.2020.129007>.

## References

- [1] G. Manda, G. Isvoranu, M.V. Comanescu, A. Manea, B. Debele Butuner, K. S. Korkmaz, The redox biology network in cancer pathophysiology and therapeutics, *Redox Biol.* 5 (2015) 347–357, <https://doi.org/10.1016/j.redox.2015.06.014>.
- [2] K.D. Weltmann, T. von Woedtke, Plasma medicine-current state of research and medical application, *Plasma Phys. Contr. Fusion* 59 (2017) 014031, <https://doi.org/10.1088/0741-3335/59/1/014031>.
- [3] X. Dai, K. Bazaka, D.J. Richard, E.R.W. Thompson, K.K. Ostrikov, The emerging role of gas plasma in oncology, *Trends Biotechnol.* 36 (2018) 1183–1198, <https://doi.org/10.1016/j.tibtech.2018.06.010>.
- [4] A. Dubuc, P. Monsarrat, F. Virard, N. Merbahi, J.-P. Sarrette, S. Laurencin-Dalicioux, S. Cousty, Use of cold-atmospheric plasma in oncology: a concise systematic review, *Ther. Adv. Med. Oncol.* 10 (2018), <https://doi.org/10.1177/1758835918786475>, 1758835918786475.
- [5] M. Keidar, A prospectus on innovations in the plasma treatment of cancer, *Phys. Plasmas* 25 (2018) 083504, <https://doi.org/10.1063/1.5034355>.
- [6] M.L. Semmler, S. Bekeschus, M. Schäfer, T. Bernhardt, T. Fischer, K. Witzke, C. Seebauer, H. Rebl, E. Grambow, B. Vollmar, J.B. Nebe, H.-R. Metelmann, T. V. Woedtke, S. Emmert, L. Boeckmann, Molecular mechanisms of the efficacy of cold atmospheric pressure plasma (CAP) in cancer treatment, *Cancers* 12 (2020) 269, <https://doi.org/10.3390/cancers12020269>.
- [7] S.U. Kalghatgi, G. Fridman, M. Cooper, G. Nagaraj, M. Peddinghaus, M. Balasubramanian, V.N. Vasilets, A.F. Gutsol, A. Fridman, G. Friedman, Mechanism of blood coagulation by nonthermal atmospheric pressure dielectric barrier discharge plasma, *IEEE Trans. Plasma Sci.* 35 (2007) 1559–1566, <https://doi.org/10.1109/TPS.2007.905953>.
- [8] S. Bekeschus, J. Brüggemeier, C. Hackbarth, T. von Woedtke, L.-I. Pardecke, J. van der Linde, Platelets are key in cold physical plasma-facilitated blood coagulation in mice, *Clin. Plasma Med.* 7-8 (2017) 58–65, <https://doi.org/10.1016/j.cpm.2017.10.001>.
- [9] G. Fridman, M. Peddinghaus, M. Balasubramanian, H. Ayan, A. Fridman, A. Gutsol, A. Brooks, Blood coagulation and living tissue sterilization by floating-electrode dielectric barrier discharge in air, *Plasma Chem. Plasma Process.* 26 (2006) 425–442, <https://doi.org/10.1007/s11090-006-9024-4>.
- [10] L. Gan, S. Zhang, D. Poorun, D. Liu, X. Lu, M. He, X. Duan, H. Chen, Medical applications of nonthermal atmospheric pressure plasma in dermatology, *JDDG: Journal der Deutschen Dermatologischen Gesellschaft* 16 (2018) 7–13, <https://doi.org/10.1111/ddg.13373>.
- [11] O. Assadian, K.J. Ousey, G. Daeschlein, A. Kramer, C. Parker, J. Tanner, D. J. Leaper, Effects and safety of atmospheric low-temperature plasma on bacterial reduction in chronic wounds and wound size reduction: a systematic review and meta-analysis, *Int. Wound J.* 16 (2019) 103–111, <https://doi.org/10.1111/iwj.12999>.
- [12] T. Bernhardt, M.L. Semmler, M. Schäfer, S. Bekeschus, S. Emmert, L. Boeckmann, Plasma medicine: applications of cold atmospheric pressure plasma in dermatology, *Oxid. Med. Cell. Longev.* 2019 (2019) 3873928, <https://doi.org/10.1155/2019/3873928>.
- [13] G.C. Kim, H.W. Lee, J.H. Byun, J. Chung, Y.C. Jeon, J.K. Lee, Dental applications of low-temperature nonthermal plasmas, *Plasma Process. Polym.* 10 (2013) 199–206, <https://doi.org/10.1002/ppap.201200065>.
- [14] S. Wu, Y. Cao, X. Lu, The state of the art of applications of atmospheric-pressure nonequilibrium plasma jets in dentistry, *IEEE Trans. Plasma Sci.* 44 (2016) 134–151, <https://doi.org/10.1109/TPS.2015.2506658>.
- [15] M. Gherardi, R. Tonini, V. Colombo, Plasma in dentistry: brief history and current status, *Trends Biotechnol.* 36 (2018) 583–585, <https://doi.org/10.1016/j.tibtech.2017.06.009>.
- [16] T. von Woedtke, A. Schmidt, S. Bekeschus, K. Wende, K.D. Weltmann, Plasma medicine: a field of applied redox biology, *In vivo (Athens, Greece)* 33 (2019) 1011–1026, <https://doi.org/10.21873/in vivo.11570>.
- [17] S. Mitra, L.N. Nguyen, M. Akter, G. Park, E.H. Choi, N.K. Kaushik, Impact of ROS generated by chemical, physical, and plasma techniques on cancer attenuation, *Cancers (Basel)* 11 (2019), <https://doi.org/10.3390/cancers11071030>.
- [18] A. Privat-Maldonado, A. Schmidt, A. Lin, K.D. Weltmann, K. Wende, A. Bogaerts, S. Bekeschus, ROS from physical plasmas: redox chemistry for biomedical therapy, *Oxid. Med. Cell. Longev.* 2019 (2019) 9062098, <https://doi.org/10.1155/2019/9062098>.
- [19] X. Lu, M. Keidar, M. Laroussi, E. Choi, E.J. Szili, K. Ostrikov, Transcutaneous plasma stress: from soft-matter models to living tissues, *Mater. Sci. Eng. R Rep.* 138 (2019) 36–59, <https://doi.org/10.1016/j.mser.2019.04.002>.
- [20] P. Lukes, E. Dolezalova, I. Sisrova, M. Clupek, Aqueous-phase chemistry and bactericidal effects from an air discharge plasma in contact with water: evidence for the formation of peroxyxynitrite through a pseudo-second-order post-discharge reaction of H<sub>2</sub>O<sub>2</sub> and HNO<sub>2</sub>, *Plasma Sources Sci. Technol.* 23 (2014) 015019, <https://doi.org/10.1088/0963-0252/23/1/015019>.
- [21] G. Busco, F. Fasani, S. Dozias, L. Ridou, C. Douat, J. P. Pouvesle, E. Robert, C. Grillon, Changes in oxygen level upon cold plasma treatments: consequences for RONS production, *IEEE Trans. Radiat. Plasma Med. Sci.* 2 (2018) 147–152, <https://doi.org/10.1109/TRPMS.2017.2775705>.
- [22] S. Reuter, J. Winter, A. Schmidt-Bleker, H. Tresp, M.U. Hammer, K.D. Weltmann, Controlling the ambient air affected reactive species composition in the effluent of an argon plasma jet, *IEEE Trans. Plasma Sci.* 40 (2012) 2788–2794, <https://doi.org/10.1109/TPS.2012.2204280>.
- [23] J.-W. Lackmann, G. Bruno, H. Jablonowski, F. Kogelheide, B. Offerhaus, J. Held, V. Schulz-von der Gathen, K. Stapelmann, T. von Woedtke, K. Wende, Nitrosylation vs. oxidation - how to modulate cold physical plasmas for biological applications, *PLoS One* 14 (2019) e0216606, <https://doi.org/10.1371/journal.pone.0216606>.
- [24] T. Darny, J.M. Pouvesle, V. Puech, C. Douat, S. Dozias, E. Robert, Analysis of conductive target influence in plasma jet experiments through helium metastable and electric field measurements, *Plasma Sources Sci. Technol.* 26 (2017), <https://doi.org/10.1088/1361-6595/aa5b15>.
- [25] A. Sobota, O. Guaitella, G.B. Sretenovic, V.V. Kovacevic, E. Slikboer, I.B. Krstic, B. M. Obradovic, M.M. Kuraica, Plasma-surface interaction: dielectric and metallic targets and their influence on the electric field profile in a kHz AC-driven He plasma jet, *Plasma Sources Sci. Technol.* 28 (2019) <https://doi.org/ARTN04500310.1088/1361-6595/ab0c6a>.
- [26] E. Simoncelli, A. Stancampiano, M. Boselli, M. Gherardi, V. Colombo, Experimental investigation on the influence of target physical properties on an impinging plasma jet, *Plasma* 2 (2019) 369–379, <https://doi.org/10.3390/plasma2030029>.
- [27] T. Darny, J.M. Pouvesle, J. Fontane, L. Joly, S. Dozias, E. Robert, Plasma action on helium flow in cold atmospheric pressure plasma jet experiments, *Plasma Sources Sci. Technol.* 26 (2017), <https://doi.org/10.1088/1361-6595/aa8877>.
- [28] D. Breden, L.L. Raja, Computational study of the interaction of cold atmospheric helium plasma jets with surfaces, *Plasma Sources Sci. Technol.* 23 (2014), <https://doi.org/10.1088/0963-0252/23/6/065020>.
- [29] H. Jablonowski, J. Santos Sousa, K.D. Weltmann, K. Wende, S. Reuter, Quantification of the ozone and singlet delta oxygen produced in gas and liquid phases by a non-thermal atmospheric plasma with relevance for medical treatment, *Sci. Rep.* 8 (2018) 12195, <https://doi.org/10.1038/s41598-018-30483-w>.
- [30] P.J. Bruggeman, M.J. Kushner, B.R. Locke, J.G.E. Gardeniens, W.G. Graham, D. B. Graves, R.C.H.M. Hofman-Caris, D. Maric, J.P. Reid, E. Ceriani, D.F. Rivas, J. E. Foster, S.C. Garrick, Y. Gorbanev, S. Hamaguchi, F. Iza, H. Jablonowski, E. Klimova, J. Kolb, F. Krcma, et al., Plasma-liquid interactions: a review and roadmap, *Plasma Sources Sci. Technol.* 25 (2016) 053002, <https://doi.org/10.1088/0963-0252/25/5/053002>.
- [31] H. Tresp, M.U. Hammer, K.-D. Weltmann, S. Reuter, Effects of atmosphere composition and liquid type on plasma-generated reactive species in biologically relevant solutions, *Plasma Med.* 3 (2013) 45–55, <https://doi.org/10.1615/PlasmaMed.2014009711>.
- [32] H. Jablonowski, A. Schmidt-Bleker, K.D. Weltmann, T. von Woedtke, K. Wende, Non-touching plasma-liquid interaction - where is aqueous nitric oxide generated? *Phys. Chem. Chem. Phys.* 20 (2018) 25387–25398, <https://doi.org/10.1039/c8cp02412j>.
- [33] K. Oehmigen, M. Mahnel, R. Brandenburg, C. Wilke, K.D. Weltmann, T. von Woedtke, The role of acidification for antimicrobial activity of atmospheric pressure plasma in liquids, *Plasma Process. Polym.* 7 (2010) 250–257, <https://doi.org/10.1002/ppap.200900077>.
- [34] J. Winter, K. Wende, K. Masur, S. Iseni, M. Dunbier, M.U. Hammer, H. Tresp, K. D. Weltmann, S. Reuter, Feed gas humidity: a vital parameter affecting a cold atmospheric-pressure plasma jet and plasma-treated human skin cells, *J. Phys. D Appl. Phys.* 46 (2013) <https://doi.org/10.1088/0022-3727/46/29/295401>.
- [35] Z. Machala, B. Tarabova, K. Hensel, E. Spetlikova, L. Sikurova, P. Lukes, Formation of ROS and RNS in water electro-sprayed through transient spark discharge in air and their bactericidal effects, *Plasma Process. Polym.* 10 (2013) 649–659, <https://doi.org/10.1002/ppap.201200113>.
- [36] R. Flyunt, A. Leitzke, G. Mark, E. Mvula, E. Reisz, R. Schick, C. von Sonntag, Determination of •OH, O<sub>2</sub>•<sup>-</sup>, and hydroperoxide yields in ozone reactions in aqueous solution†, *J. Phys. Chem. B* 107 (2003) 7242–7253, <https://doi.org/10.1021/jp022455b>.
- [37] V.S.S.K. Kondeti, C.Q. Phan, K. Wende, H. Jablonowski, U. Gangal, J.L. Granick, R. C. Hunter, P.J. Bruggeman, Long-lived and short-lived reactive species produced by a cold atmospheric pressure plasma jet for the inactivation of *Pseudomonas aeruginosa* and *Staphylococcus aureus*, *Free Radic. Biol. Med.* 124 (2018) 275–287, <https://doi.org/10.1016/j.freeradbiomed.2018.05.083>.
- [38] G. Bruno, T. Heusler, J.-W. Lackmann, T. von Woedtke, K.-D. Weltmann, K. Wende, Cold physical plasma-induced oxidation of cysteine yields reactive sulfur species (RSS), *Clin. Plasma Med.* 14 (2019) 100083, <https://doi.org/10.1016/j.cpm.2019.100083>.
- [39] F. Yang, R. Zhang, J. He, Z. Abliz, Development of a liquid chromatography/electrospray ionization tandem mass spectrometric method for the determination of hydroxyl radical, *Rapid Commun. Mass Spectrom.* 21 (2007) 107–111, <https://doi.org/10.1002/rcm.2815>.
- [40] Y. Wang, H. Xu, J. Zhang, G. Li, Electrochemical sensors for clinic analysis, *Sensors (Basel, Switzerland)* 8 (2008) 2043–2081, <https://doi.org/10.3390/s8042043>.
- [41] N. Bunyakul, A.J. Baeumner, Combining electrochemical sensors with miniaturized sample preparation for rapid detection in clinical samples, *Sensors (Basel)* 15 (2014) 547–564, <https://doi.org/10.3390/s150100547>.

- [42] M.H. Naveen, N.G. Gurudatt, Y.B. Shim, Applications of conducting polymer composites to electrochemical sensors: a review, *Appl. Mater. Today* 9 (2017) 419–433, <https://doi.org/10.1016/j.apmt.2017.09.001>.
- [43] K. Dhara, D.R. Mahapatra, Recent advances in electrochemical nonenzymatic hydrogen peroxide sensors based on nanomaterials: a review, *J. Mater. Sci.* 54 (2019) 12319–12357, <https://doi.org/10.1007/s10853-019-03750-y>.
- [44] D. Runsewe, T. Betancourt, J.A. Irvin, Biomedical application of electroactive polymers in electrochemical sensors: a review, *Materials (Basel)* 12 (2019) 29, <https://doi.org/10.3390/ma12162629>.
- [45] Y.Z. Wang, S.S. Hu, A novel nitric oxide biosensor based on electropolymerization poly(toluidine blue) film electrode and its application to nitric oxide released in liver homogenate, *Biosens. Bioelectron.* 22 (2006) 10–17, <https://doi.org/10.1016/j.bios.2005.11.012>.
- [46] K. Thenmozhi, S.S. Narayanan, Covalently immobilized toluidine blue/sol-gel film electrode for the amperometric determination of hydrogen peroxide, *J. Indian Chem. Soc.* 92 (2015) 443–446.
- [47] B. Sriram, T.W. Chen, S.M. Chen, K.K. Rani, R. Devasenathipathy, S.F. Wang, Fabrication of poly (Toluidine blue O) functionalized multiwalled carbon nanotubes on glassy carbon electrode for hydrazine detection, *Int. J. Electrochem. Sci.* 13 (2018) 4901–4910, <https://doi.org/10.20964/2018.05.65>.
- [48] D. Gligor, A. Walcarius, Glassy carbon electrode modified with a film of poly (Toluidine Blue O) and carbon nanotubes for nitrite detection, *J. Solid State Electrochem.* 18 (2014) 1519–1528, <https://doi.org/10.1007/s10008-10013-2365-z>.
- [49] S.-M. Chen, G.-H. Chuang, V.S. Vasantha, Preparation and electrocatalytic properties of the TBO/naftion chemically-modified electrodes, *J. Electroanal. Chem.* 588 (2006) 235–243, <https://doi.org/10.1016/j.jelechem.2006.01.001>.
- [50] Z. Nasri, E. Shams, M. Ahmadi, Direct modification of a glassy carbon electrode with toluidine blue diazonium salt: application to NADH determination and biosensing of ethanol, *Electroanalysis* 25 (2013) 1917–1925, <https://doi.org/10.1002/elan.201300062>.
- [51] C.C.W. Verlaack, W. Van Boxtem, A. Bogaerts, Transport and accumulation of plasma generated species in aqueous solution, *Phys. Chem. Chem. Phys.* 20 (2018) 6845–6859, <https://doi.org/10.1039/c7cp07593f>.
- [52] M.S. Mann, R. Tiede, K. Gavenis, G. Daeschlein, R. Bussiahn, K.-D. Weltmann, S. Emmert, T. von Woedtke, R. Ahmed, Introduction to DIN-specification 91315 based on the characterization of the plasma jet kINPen® MED, *Clin. Plasma Med.* 4 (2016) 35–45, <https://doi.org/10.1016/j.cpm.2016.06.001>.
- [53] S. Reuter, H. Tresp, K. Wende, M.U. Hammer, J. Winter, K. Masur, A. Schmidt-Bleker, K.D. Weltmann, From RONS to ROS: tailoring plasma jet treatment of skin cells, *IEEE Trans. Plasma Sci.* 40 (2012) 2986–2993, <https://doi.org/10.1109/Tps.2012.2207130>.
- [54] M. Delamar, R. Hitmi, J. Pinson, J.M. Saveant, Covalent modification of carbon surfaces by grafting of functionalized aryl radicals produced from electrochemical reduction of diazonium salts, *J. Am. Chem. Soc.* 114 (1992) 5883–5884, <https://doi.org/10.1021/ja00040a074>.
- [55] L. Bundscherer, S. Bekeschus, H. Tresp, S. Hasse, S. Reuter, K.-D. Weltmann, U. Lindequist, K. Masur, Viability of human blood leukocytes compared with their respective cell lines after plasma treatment, *Plasma Med.* 3 (2013) 71–80, <https://doi.org/10.1615/PlasmaMed.2013008538>.
- [56] Y. Gorbanev, J. Van der Paal, W. Van Boxtem, S. Dewilde, A. Bogaerts, Reaction of chloride anion with atomic oxygen in aqueous solutions: can cold plasma help in chemistry research? *Phys. Chem. Chem. Phys.* 21 (2019) 4117–4121, <https://doi.org/10.1039/c8cp07550f>.
- [57] D.W. O'Sullivan, M. Tyree, The kinetics of complex formation between Ti(IV) and hydrogen peroxide, *Int. J. Chem. Kinet.* 39 (2007) 457–461, <https://doi.org/10.1002/kin.20259>.
- [58] Y. Guo, Q. Ma, F. Cao, Q. Zhao, X. Ji, Colorimetric detection of hypochlorite in tap water based on the oxidation of 3,3',5,5'-tetramethyl benzidine, *Anal. Methods* 7 (2015) 4055–4058, <https://doi.org/10.1039/C5AY00735F>.
- [59] D. Belanger, J. Pinson, Electrografting: a powerful method for surface modification, *Chem. Soc. Rev.* 40 (2011) 3995–4048, <https://doi.org/10.1039/c0cs00149j>.
- [60] J. Pinson, F. Podvorica, Attachment of organic layers to conductive or semiconductive surfaces by reduction of diazonium salts, *Chem. Soc. Rev.* 34 (2005) 429–439, <https://doi.org/10.1039/b406228k>.
- [61] R. Mazeikiene, G. Niaura, O. Eicher-Lorka, A. Malinauskas, Raman spectroelectrochemical study of Toluidine Blue, adsorbed and electropolymerized at a gold electrode, *Vib. Spectrosc.* 47 (2008) 105–112, <https://doi.org/10.1016/j.vibspec.2008.02.018>.
- [62] R. Mazeikiene, G. Niaura, A. Malinauskas, Raman spectroelectrochemical study of electrochemical decomposition of poly(neutral red) at a gold electrode, *J. Colloid Interface Sci.* 336 (2009) 195–199, <https://doi.org/10.1016/j.jcis.2009.03.094>.
- [63] K. Wende, T. von Woedtke, K.D. Weltmann, S. Bekeschus, Chemistry and biochemistry of cold physical plasma derived reactive species in liquids, *Biol. Chem.* 400 (2018) 19–38, <https://doi.org/10.1515/hsz-2018-0242>.
- [64] A.M. Hirst, F.M. Frame, M. Arya, N.J. Maitland, D. O'Connell, Low temperature plasmas as emerging cancer therapeutics: the state of play and thoughts for the future, *Tumour Biol.* (2016), <https://doi.org/10.1007/s13277-016-4911-4917>.
- [65] M. Kimura, T. Suzuki, Y. Ogata, Hypochlorite oxidation of ammonia - effective removal of ammonia from wastewater by uv-irradiation, *Bull. Chem. Soc. Jpn.* 53 (1980) 3198–3201, <https://doi.org/10.1246/bcsj.53.3198>.
- [66] Z.T. How, I. Kristiana, F. Busetti, K.L. Linge, C.A. Joll, Organic chloramines in chlorine-based disinfected water systems: a critical review, *J. Environ. Sci.* 58 (2017) 2–18, <https://doi.org/10.1016/j.jes.2017.05.025>.
- [67] M. Duennbier, A. Schmidt-Bleker, J. Winter, M. Wolfram, R. Hippler, K. D. Weltmann, S. Reuter, Ambient air particle transport into the effluent of a cold atmospheric-pressure argon plasma jet investigated by molecular beam mass spectrometry, *J. Phys. D Appl. Phys.* 46 (2013) 435203, <https://doi.org/10.1088/0022-3727/46/43/435203>.
- [68] K. Wende, P. Williams, J. Dalluge, W.V. Gaens, H. Aboubakr, J. Bischof, T. von Woedtke, S.M. Goyal, K.D. Weltmann, A. Bogaerts, K. Masur, P.J. Bruggeman, Identification of the biologically active liquid chemistry induced by a nonthermal atmospheric pressure plasma jet, *Biointerphases* 10 (2015) 029518, <https://doi.org/10.1116/1.4919710>.
- [69] S. Bekeschus, K. Wende, M.M. Hefny, K. Rodder, H. Jablonowski, A. Schmidt, T. von Woedtke, K.D. Weltmann, J. Benedikt, Oxygen atoms are critical in rendering THP-1 leukaemia cells susceptible to cold physical plasma-induced apoptosis, *Sci. Rep.* 7 (2017), <https://doi.org/10.1038/s41598-017-03131-y>.
- [70] S. Maheux, D. Duda, T. Belmonte, C. Penny, H.M. Cauchie, F. Clement, P. Choquet, Formation of ammonium in saline solution treated by nanosecond pulsed cold atmospheric microplasma: a route to fast inactivation of E-coli bacteria, *RSC Adv.* 5 (2015) 42135–42140, <https://doi.org/10.1039/c5ra01109d>.
- [71] G. Bauer, D. Sersenová, D.B. Graves, Z. Machala, Cold atmospheric plasma and plasma-activated medium trigger RONS-based tumor cell apoptosis, *Sci. Rep.* 9 (2019) 14210, <https://doi.org/10.1038/s41598-019-50291-0>.
- [72] A. Schmidt, K. Rödder, S. Hasse, K. Masur, L. Toups, C.H. Lillig, T. von Woedtke, K. Wende, S. Bekeschus, Redox-regulation of activator protein 1 family members in blood cancer cell lines exposed to cold physical plasma-treated medium, *Plasma Process. Polym.* 13 (2016) 1179–1188, <https://doi.org/10.1002/ppap.201600090>.
- [73] D. Yan, H. Cui, W. Zhu, A. Talbot, L.G. Zhang, J.H. Sherman, M. Keidar, The strong cell-based hydrogen peroxide generation triggered by cold atmospheric plasma, *Sci. Rep.* 7 (2017) 10831, <https://doi.org/10.1038/s41598-017-11480-x>.

**Zahra Nasri** received her Ph.D. degree in analytical chemistry in 2013 from the University of Isfahan, Iran. Her research activity concerned with the development of sensors and biosensors for different applications. Currently, she is a postdoctoral researcher at Leibniz Institute for Plasma Science and Technology (INP) Greifswald, Germany. Her current research area is focused on cold physical plasma liquid interaction to investigate relevant species and parameters responsible for the biological effects of plasma.

**Giuliana Bruno** received her BSc degree (Pharmaceutical Sciences and Technologies) in 2014 from the University of Salerno (Italy), and her MSc degree (Medical and Pharmaceutical Biotechnologies) in 2016 from the University of Sannio (Italy). She is currently a third year PhD student at the Leibniz Institute for Plasma Science and Technology (Greifswald, Germany). Her research activity concerns the study of the biochemical effects generated by the interaction between cold plasmas and small biomolecules in solution.

**Sander Bekeschus** is currently head of Department of Plasma-Redox-Effects and principal researcher in the division of ZIK plasmatis, Leibniz Institute for Plasma Science and Technology (INP), Germany. He received the MSc (Human Biology with Major in Immunology) degree from the University of Greifswald, Germany, and his PhD in 2015 from the same University. His current research areas are gas plasma research in the biomedical context of health and disease and the associated immunological consequences.

**Klaus-Dieter Weltmann** received his doctoral degree (Dr. rer. nat.) in Theoretical Physics from University Greifswald. Since 2003 he has been director and chairman of the board of the Institute for Plasma Science and Technology (INP) Greifswald and head of the research department Environment & Health. He is also C4 / W3 professor at the University of Greifswald for experimental physics and guest professor at the Polytechnic Institute of New York University.

**Thomas von Woedtke** received the doctoral degree (Dr. rer. nat.) and the Habilitation degree (Dr. rer. nat. habil.) in Pharmaceutical Technology from the University of Greifswald, Germany. Currently he is Research Program Manager Plasma Medicine at the Leibniz Institute for Plasma Science and Technology (INP) Greifswald and Member of the Board of INP. He holds a professorship for Plasma Medicine at Greifswald University Medicine.

**Kristian Wende** received his MSc degree (natural compound chemistry) in 1998 and the Ph.D. degree (natural compound analytics and toxicology) in 2003 from the University of Greifswald. He is a research group leader at the Leibniz Institute for Plasma Science and Technology in Greifswald, Germany. His current research comprises analytical and biological methods to determine biomolecule oxidation in the context of redox biology.